

NASA/TM-2014-218545



Nondestructive Evaluation (NDE) for Inspection of Composite Sandwich Structures

*Joseph N. Zalameda and F. Raymond Parker
Langley Research Center, Hampton, Virginia*

November 2014

NASA STI Program . . . in Profile

Since its founding, NASA has been dedicated to the advancement of aeronautics and space science. The NASA scientific and technical information (STI) program plays a key part in helping NASA maintain this important role.

The NASA STI program operates under the auspices of the Agency Chief Information Officer. It collects, organizes, provides for archiving, and disseminates NASA's STI. The NASA STI program provides access to the NASA Aeronautics and Space Database and its public interface, the NASA Technical Report Server, thus providing one of the largest collections of aeronautical and space science STI in the world. Results are published in both non-NASA channels and by NASA in the NASA STI Report Series, which includes the following report types:

- **TECHNICAL PUBLICATION.** Reports of completed research or a major significant phase of research that present the results of NASA Programs and include extensive data or theoretical analysis. Includes compilations of significant scientific and technical data and information deemed to be of continuing reference value. NASA counterpart of peer-reviewed formal professional papers, but having less stringent limitations on manuscript length and extent of graphic presentations.
- **TECHNICAL MEMORANDUM.** Scientific and technical findings that are preliminary or of specialized interest, e.g., quick release reports, working papers, and bibliographies that contain minimal annotation. Does not contain extensive analysis.
- **CONTRACTOR REPORT.** Scientific and technical findings by NASA-sponsored contractors and grantees.

- **CONFERENCE PUBLICATION.** Collected papers from scientific and technical conferences, symposia, seminars, or other meetings sponsored or co-sponsored by NASA.
- **SPECIAL PUBLICATION.** Scientific, technical, or historical information from NASA programs, projects, and missions, often concerned with subjects having substantial public interest.
- **TECHNICAL TRANSLATION.** English-language translations of foreign scientific and technical material pertinent to NASA's mission.

Specialized services also include organizing and publishing research results, distributing specialized research announcements and feeds, providing information desk and personal search support, and enabling data exchange services.

For more information about the NASA STI program, see the following:

- Access the NASA STI program home page at <http://www.sti.nasa.gov>
- E-mail your question to help@sti.nasa.gov
- Fax your question to the NASA STI Information Desk at 443-757-5803
- Phone the NASA STI Information Desk at 443-757-5802
- Write to:
STI Information Desk
NASA Center for AeroSpace Information
7115 Standard Drive
Hanover, MD 21076-1320

NASA/TM-2014-218545



Nondestructive Evaluation (NDE) for Inspection of Composite Sandwich Structures

*Joseph N. Zalameda and F. Raymond Parker
Langley Research Center, Hampton, Virginia*

National Aeronautics and
Space Administration

Langley Research Center
Hampton, Virginia 23681-2199

November 2014

Available from:

NASA Center for AeroSpace Information
7115 Standard Drive
Hanover, MD 21076-1320
443-757-5802

Abstract

Composite honeycomb structures are widely used in aerospace applications due to their low weight and high strength advantages. Developing nondestructive evaluation (NDE) inspection methods are essential for their safe performance. Flash thermography is a commonly used technique for composite honeycomb structure inspections due to its large area and rapid inspection capability. Flash thermography is shown to be sensitive for detection of face sheet impact damage and face sheet to core disbond. Data processing techniques, using principal component analysis to improve the defect contrast, are discussed. Limitations to the thermal detection of the core are investigated. In addition to flash thermography, X-ray computed tomography is used. The aluminum honeycomb core provides excellent X-ray contrast compared to the composite face sheet. The X-ray CT technique was used to detect impact damage, core crushing, and skin to core disbonds. Additionally, the X-ray CT technique is used to validate the thermography results.

Nomenclature

V	= temperature
l	= thickness
K	= thermal conductivity
f	= heat flux
α	= thermal diffusivity
s	= Laplace transform complex argument

Introduction

Composite honeycomb structures continue to be used widely in aerospace applications due to low weight and high strength requirements. There is a growing interest in the application of thermal methods for nondestructive evaluation (NDE) of composite sandwich structures [1-3]. Some of the advantages of thermal NDE are noncontact, rapid, capable of imaging large areas, applicable to complex geometries, and quantitative. The technique is safe where only a small amount of heat is applied to the surface of the structure. Thermography has shown good potential for detection of various defects in composite structures. Defects such as delaminations, disbonds, gross porosity, and fiber volume fraction variations are detectable using thermography. X-ray computed tomography (CT) is also used to detect defects in sandwich structures [4]. The X-ray CT inspection results provide a true volumetric measurement of the damage, however the inspection must be performed within a radiation enclosure. The aluminum honeycomb core provides excellent X-ray contrast compared to the composite face sheets and therefore, is an ideal inspection technique. The X-ray system is used to detect impact damage, core crushing, and skin to core disbonds.

Specific to composite honeycomb structures, face sheet delaminations, face sheet to core disbonds, and core crushing are defects of interest. Typically the composite face sheets are relatively thin compared to the overall thickness and therefore, thermography is effective for detection of face sheet delaminations. Detection of the face sheet to core disbonds is also critical. Under load, face sheet to core disbonds can grow leading to disbond buckling failure which can lead to catastrophic structural failure [5]. Both thermography and X-ray CT have the potential to detect face sheet to core disbonds. The thermal detection limitations of face sheet to core disbonds are investigated using analytical and finite element thermal modeling.

Flash thermography results are presented on composite honeycomb samples with face sheet delaminations, face sheet to core disbonds, and core crushing. The thermal results are compared to the X-ray CT measurements. Thermal modeling is used to optimize the inspection. The thermal modeling consisted of a 1-dimensional (1-D) analytic model and 2-dimensional (2-D) finite element model. The 1-D analytical model is used to provide an understanding of the effect of the adhesive between the face sheet and core. The 2-D finite element model is used for two purposes: first to determine the optimal thermal processing parameters for detection of face sheet delamination damage and face sheet to core disbonds and second to determine the thermal detection limitations caused by the face sheet to core thickness ratio. This model is also used for differentiating between impact damage and face sheet disbonds using early time and late time analysis. X-ray CT is used to image the skin to core disbond and impact damage areas by viewing averaged image data through-the-thickness. The core crushed areas are detected by measuring the deviation of the core away from the non-damaged side.

Sample Configuration

The configuration of the composite sandwich samples studied is shown in Figure 1. The sandwich structure is comprised of an aluminum hexagonal core with outer graphite plain weave composite face sheets. The core thickness is 2.54 cm and the composite face sheet thickness is approximately 0.1 cm. The core cell wall thickness is

approximately 0.02 cm with a cell size of 0.32 cm. The ratio of the face sheet to core wall thickness is 5 to 1.

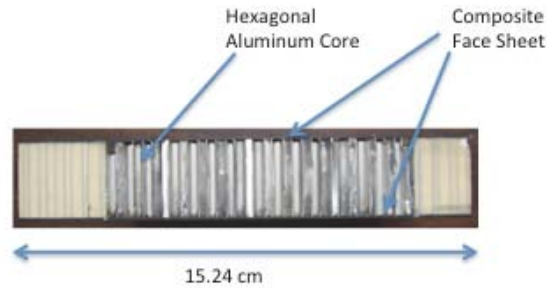


Figure 1. Typical configuration of composite face sheet with aluminum core.

Flash Thermography

Thermographic single side flash inspection data were acquired using a commercially available thermal inspection system. The thermal inspection system uses two flash lamps that are mounted within a hood to contain the flash, as shown in Figure 2. The flash power is provided from two power supplies delivering 4.8 kJ of energy to the flash tubes. The flash duration is typically less than 10 milliseconds and is instantaneous compared to the frame rate of the camera and the thermal response time of the composite [6]. An infrared camera was used to record the surface temperature response. The camera operates in the mid infrared band with a pixel resolution of 640x512. The camera sensitivity or noise equivalent temperature difference, quoted by the manufacturer, is less than 0.02 Kelvin. The camera is configured with a 25 mm germanium optical lens. The data were acquired at 60 Hz for 720 frames. The total acquisition time was 12 seconds.

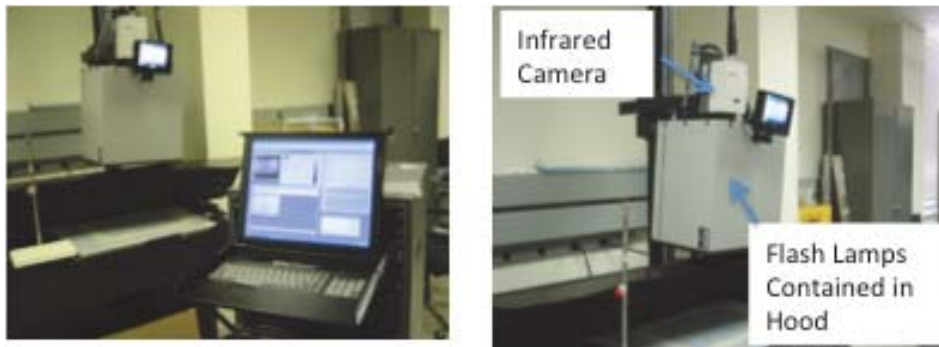


Figure 2. Thermal inspection system with flash lamps contained in hood.

Thermal Modeling

The thermal modeling efforts included a 1-D approach to investigate the effects of the adhesive between the face sheet and core. A multi-layer 1-D thermal model was used by comparing the difference in the thermal response between the face sheet bonded directly to the core and a thin layer of adhesive between the face sheet and core. From these results, a 2-D finite element model was configured similar to the right

image of Figure 3 using a “T” configuration. This was used to study the effect of the lateral heat flow in reducing thermal contrast for imaging a core disbond. Simulated camera noise, determined from actual thermal data, was added to the model results. An X-ray CT image showing the aluminum core bonded to a composite face sheet is shown in the left image of Figure 3. For both of these models, the fillet bonds between the core and adhesive along the length of the core wall were not considered.

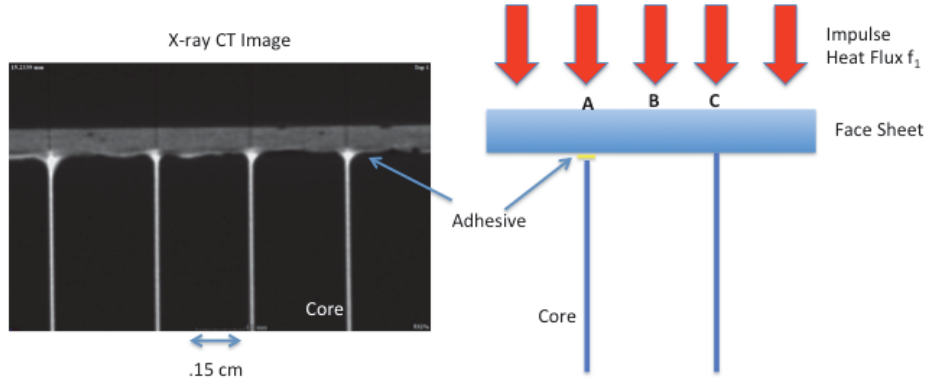


Figure 3. X-ray CT image (left) showing actual thermal configuration of attached core to the face sheet and thermal model configuration (right).

1-D Modeling

The 1-D analytical model provided an understanding of the effect of the adhesive between the face sheet and core and is given in equation (1) [7]. The multilayered model includes the face sheet composite layer, the adhesive layer and the core layer. A contrast function is defined by the temperature difference response to impulse flux heating at the surface between points A, B, and C as shown in Figure 3. For point A, the 1-D analytical model contains 3 layers: the face sheet, the adhesive, and the core, equation (1). For points B and C the analytical model contains 1 layer (face sheet layer only) and 2 layers (face sheet and the core), equations (2) and (3) respectively. The equations are given below as:

$$\begin{bmatrix} V_1 \\ 0 \end{bmatrix} = \begin{bmatrix} \cosh [q_2 l_2] & -\frac{1}{K_{core} q_2} \sinh [q_2 l_2] \\ -K_{core} q_2 \sinh [q_2 l_2] & \cosh [q_2 l_2] \end{bmatrix} \begin{bmatrix} 1 \\ 0 \end{bmatrix} - \frac{1}{K_{adhesive}} \begin{bmatrix} \cosh [q_1 l_1] & -\frac{1}{K_{comp} q_1} \sinh [q_1 l_1] \\ -K_{comp} q_1 \sinh [q_1 l_1] & \cosh [q_1 l_1] \end{bmatrix} \begin{bmatrix} V_A \\ f_1 \end{bmatrix} \quad (1)$$

$$\begin{bmatrix} V_2 \\ 0 \end{bmatrix} = \begin{bmatrix} \cosh [q_1 l_1] & -\frac{1}{K_{comp} q_1} \sinh [q_1 l_1] \\ -K_{comp} q_1 \sinh [q_1 l_1] & \cosh [q_1 l_1] \end{bmatrix} \begin{bmatrix} V_B \\ f_1 \end{bmatrix} \quad (2)$$

$$\begin{bmatrix} V_3 \\ 0 \end{bmatrix} = \begin{bmatrix} \cosh [q_2 l_2] & -\frac{1}{K_{core} q_2} \sinh [q_2 l_2] \\ -K_{core} q_2 \sinh [q_2 l_2] & \cosh [q_2 l_2] \end{bmatrix} \begin{bmatrix} \cosh [q_1 l_1] & -\frac{1}{K_{comp} q_1} \sinh [q_1 l_1] \\ -K_{comp} q_1 \sinh [q_1 l_1] & \cosh [q_1 l_1] \end{bmatrix} \begin{bmatrix} V_C \\ f_1 \end{bmatrix} \quad (3)$$

$$\text{where } q_1 = \sqrt{\frac{s}{\alpha_{comp}}} \quad \text{and} \quad q_2 = \sqrt{\frac{s}{\alpha_{core}}}$$

The model can be solved analytically in the Laplace domain [8] where V_A , V_B and V_C are the 3 layer, 1 layer, and 2 layer surface temperature responses in the Laplace domain respectively, f_1 is the instantaneous heat flux input estimated to be approximately 1 cal/cm^2 [9], l_1 is the face sheet composite layer thickness = 0.1 cm , l_2 is the core layer thickness = 2.54 cm , K_{comp} is the composite thermal conductivity = $0.0021 \text{ cal/cm sec } ^\circ\text{C}$, K_{aluminum} is the aluminum thermal conductivity = $0.33 \text{ cal/cm sec } ^\circ\text{C}$, a_{core} is the composite thermal diffusivity = $0.004 \text{ cm}^2/\text{sec}$, a_{aluminum} is the aluminum thermal diffusivity = $0.53 \text{ cm}^2/\text{sec}$, K_{adhesive} is the adhesive thermal conductivity = $0.0006 \text{ cal/cm sec } ^\circ\text{C}$, l_{adhesive} is the estimated adhesive thickness = 0.001 cm [10], and s is the Laplace complex argument. The temperature results are normalized before taking the difference. The results are shown in Figure 4 where the contrast between the model with adhesive and no adhesive ($V_A - V_C$) is plotted. In addition, the difference between the face sheet only and face sheet and core ($V_B - V_C$) is plotted for the core contrast. Compared to the core contrast the adhesive difference response is minimal.

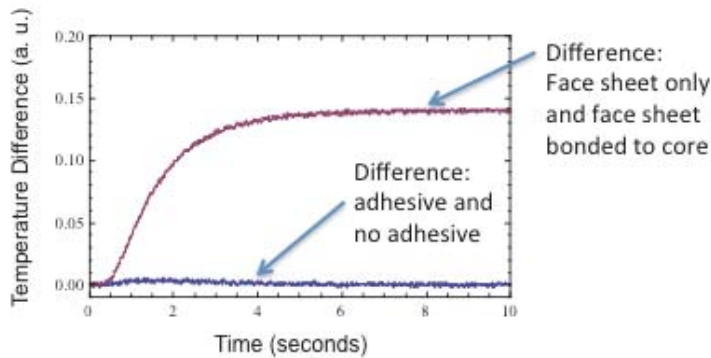


Figure 4. 1-D model temperature difference of adhesive and no adhesive compared to face sheet and face sheet and core.

2-D Finite Element Modeling

The 2-D finite element method (FEM), via a commercially available software package [11], was used to determine the thermal detection limitations caused by the face sheet to core thickness ratio. The face sheet thickness to core thickness ratios studied were 4:1, 5:1, 6:1, 7:1 and 8:1. These models were simplified using the face sheet bonded directly to the core (no adhesive) based on the 1-D results. An example finite element analysis model of a composite face sheet with aluminum core is shown in Figure 5. The 2-D model contains 1038 elements and 620 nodes. The face sheet thickness is 0.1 cm and the aluminum core cell wall thickness is 0.02 cm . The ratio of the face sheet to core thickness is 5:1. The width of the face sheet is 0.5 cm and the length of the core is 0.4 cm , as shown in Figure 5. The surface temperature (room temperature subtracted) as a function of time is also shown in Figure 5 (right plot). For early times around 0.3 seconds there is no contrast caused by the core. This reveals that defects within the face sheet can be detected around this time and therefore can be differentiated from core defects. Later in time, around 0.97 seconds, the aluminum core lowers the temperature at the face sheet surface over the core. The temperature contrast fades away around 8.3 seconds. Figure 6 shows a comparison between the 2-D FEM and the 1-D analytical model results. For early times up to around 0.75 seconds, there is fairly good agreement between the 2 models. Past 0.75 seconds the models diverge and as expected the 2-D model would predict lower temperature contrast since the lateral heat flow is taken into account. Comparisons to 2-D model results, with camera noise added, of the contrast evolution vs. time for various face sheet to core cell wall thickness ratios are shown in the right plot of Figure 6. The temperature difference was calculated

by subtracting a point over the core from a point away from the core. The core wall thickness is 0.020 cm and the thickness of the face sheet values are 0.08, 0.10, 0.12, 0.14, and 0.16 cm, resulting in face sheet thickness to core thickness ratios of 4:1, 5:1, 6:1, 7:1 and 8:1 respectively. The temperature difference is barely above the noise for the 8:1 ratio configuration indicating a face sheet to core disbond would not be detectable.

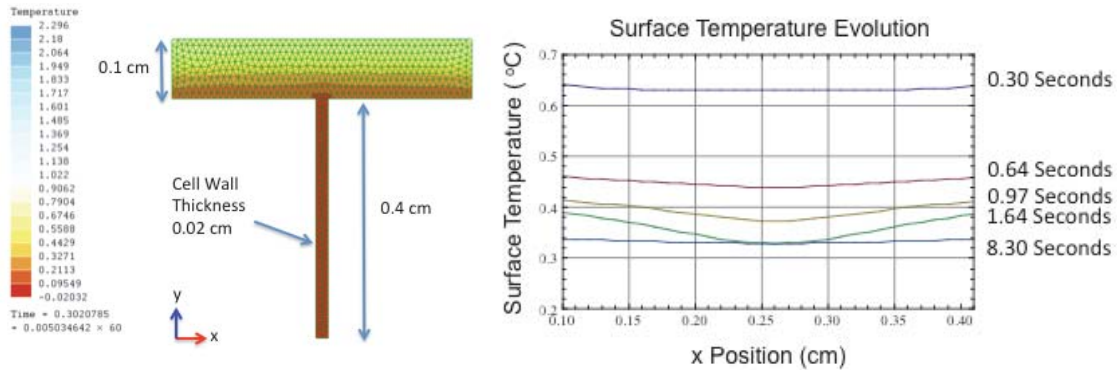


Figure 5. Finite element model of a composite face sheet with aluminum core (left image) and corresponding surface temperature evolution (right plot).

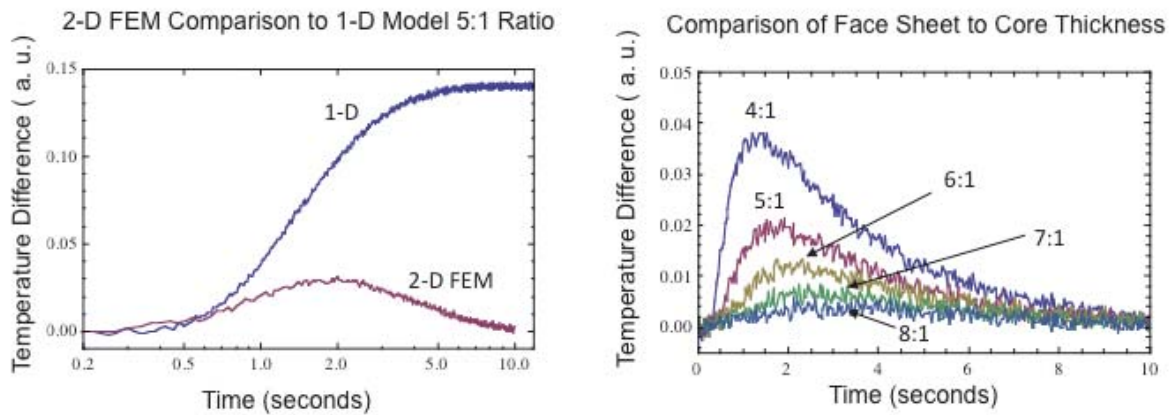


Figure 6. Contrast evolution comparison of 2-D finite element model comparison to 1-D analytical model (left plot) and temperature difference comparison of face sheet to core cell wall thickness ratios (right plot).

Data Processing

Principal component analysis (PCA) is common for processing of thermal data [12,13]. This algorithm is based on decomposition of the thermal data into its principal components or eigenvectors. Singular value decomposition is a routine used to find the singular values and corresponding eigenvectors of a matrix. Since thermal NDE signals are slowly decaying waveforms, the predominant variations of the entire data set are usually contained in the first or second eigenvectors, and thus account for most of the data variance of interest. The PCA is computed by defining a data matrix A , where the time variations are along the columns and the spatial image pixel points are row-wise. The matrix A is adjusted by subtracting the mean along the time dimension. The matrix A can then be decomposed using singular value decomposition as:

$$A^T A = U * \Gamma^2 * U^T \quad (4)$$

where Γ is a diagonal matrix containing the squares of the singular values and U is an orthogonal matrix, which contains the basis functions or eigenvectors describing the time variations. The eigenvectors can be obtained from the columns of U . The PCA image is calculated by dot product multiplication of the selected eigenvector times the temperature response (data matrix A), pixel by pixel. Typically the first or second eigenvector PCA image provides good contrast for defect detection. The first eigenvector is dominated by the transient cool down of the face sheet layer and is more suited for early time detection of face sheet delamination. The second eigenvector is less dominant and defines the temporal contrast evolution of the face sheet bonded to the core. This is shown in Figure 7 where the 2nd eigenvectors, determined from the 2-D model data for each of the thickness to core ratios, are plotted for comparison (no camera noise added). The maximum contrast point moves later in time due to the increases in the face sheet thickness, as expected. This indicates the 2nd eigenvector is the best candidate for imaging the face sheet to core disbond regions. Also the maximum contrast time determined from the 2nd eigenvectors are different compared to the maximum time determined from the difference calculation with no camera noise added (see Table 1 in Figure 7). While both agree that with increasing face sheet thickness the maximum point moves slightly later in time; the maximum contrast time determined from the 2nd eigenvector is more accurate because all the surface points are used from the model instead of only the 2 surface points used in the difference calculation. Also shown in Figure 7, the 8:1 ratio eigenvector curve does not have a clear maximum point, thus indicating the core response is not as dominant in the data and cannot be detected as confirmed by the 8:1 ratio temperature difference plot in Figure 6 (especially with camera noise added).

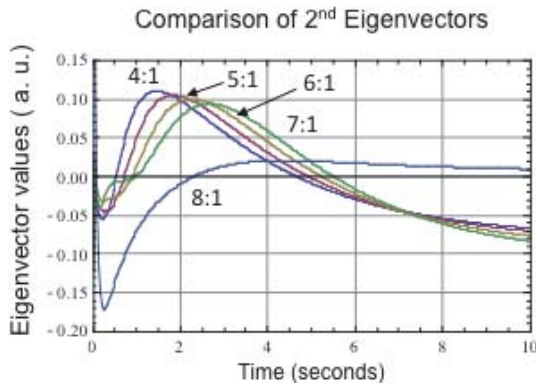


Table 1. Comparison of maximum contrast times.

Thickness to Core Ratio	Temperature Difference Max Contrast Time (seconds)	2 nd Eigenvector Local Max Time Contrast (seconds)
4:1	1.31	1.47
5:1	1.70	1.84
6:1	2.17	2.24
7:1	2.61	2.68
8:1	3.04	4.35

Figure 7. 2nd Eigenvectors determined from the 2-D FEM results (left plot) and table of maximum contrast times determined from temperature difference calculations (from Figure 6) and the local maximum contrast time from 2nd eigenvector calculations.

X-ray Computed Tomography (CT) System

The advanced micro-focus X-ray system used in this study is shown in Figure 8. This system is capable of resolving details down to 5 microns, and with magnifications up to

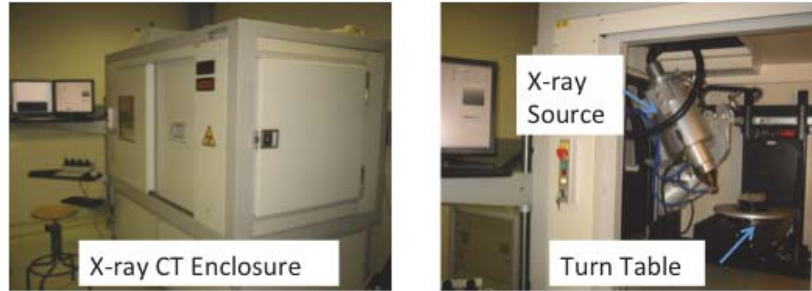


Figure 8. X-ray CT system used for sandwich structure inspections.

160 times. The X-ray source voltage can be varied from 25 to 225 kilovolts. The detector array size is 2,000 x 2,000 with a 200 μ pitch. The sample can be manipulated with 5 axes of freedom, while continuously viewing the image on a monitor. Defects can be rapidly located, zooming in for detailed analysis. The system is contained in a radiation enclosure, with X-ray, manipulator and imaging controls housed in a separate control console. Sample sizes can range up to 25.4 x 25.4 cm.

Comparison of Thermography to Computed Tomography X-ray

Based on the 2-D modeling results from sections 3.2 and 4.1, an early time window can be used for detection of defects within the composite face sheet. A late time window can be used to detect a face sheet to core disbond. Shown in Figure 9 is an early time (0.33 – 1.5 seconds) PCA image of a composite honeycomb sample with impact damage delamination defects (7 total impacts). The impact damage shows up as lighter

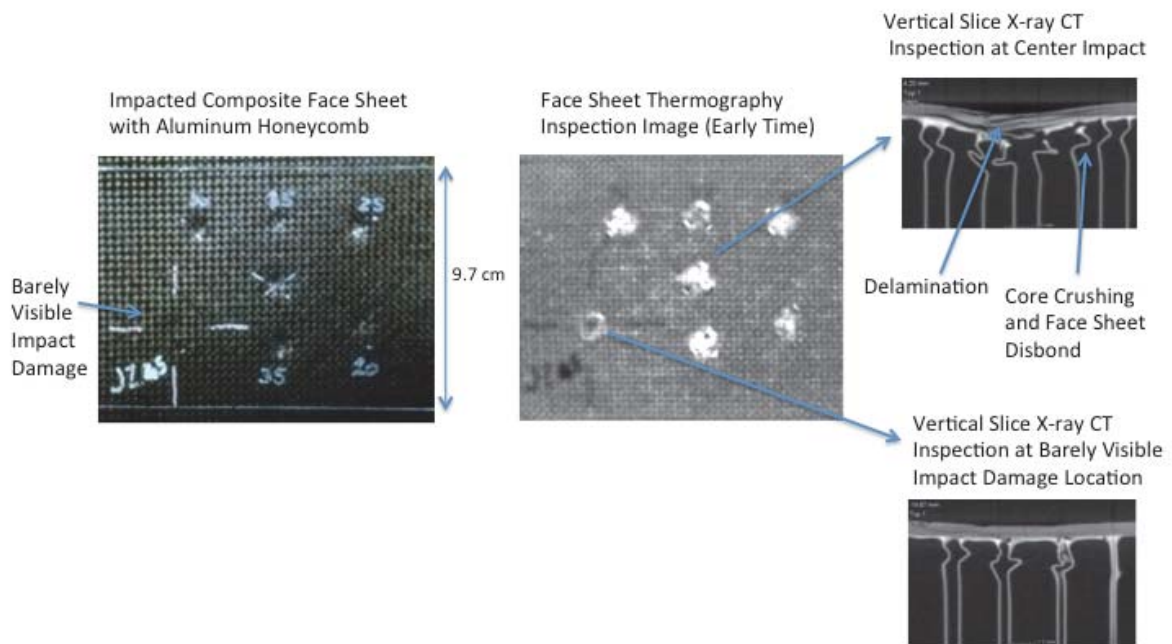


Figure 9. Photograph of impacted sandwich structure (left image) and early time thermography inspection results (middle image) along with X-ray CT (right images).

regions. The X-ray CT images show the core still attached to the face sheet with some core crushing. The PCA image was calculated from the first eigenvector. A comparison of the early time and late time (1.5 – 8.3 seconds) PCA images to X-ray CT inspection images are shown in Figure 10. There is good qualitative agreement between the thermography inspection image (early time analysis) compared to the X-ray CT image for detection of impact damage. Figure 11 shows the areas of crushed core using X-ray CT. The crushed core areas are determined by locating the core edges just below the back face sheet and following the edges toward the front surface until they deviated by three pixels from a linear fit and then traced back to a one pixel deviation; there are minor core deformations deeper into the core that are ignored. The crushed core areas, as shown in Figures 9 and 11, are not detectable with thermography.

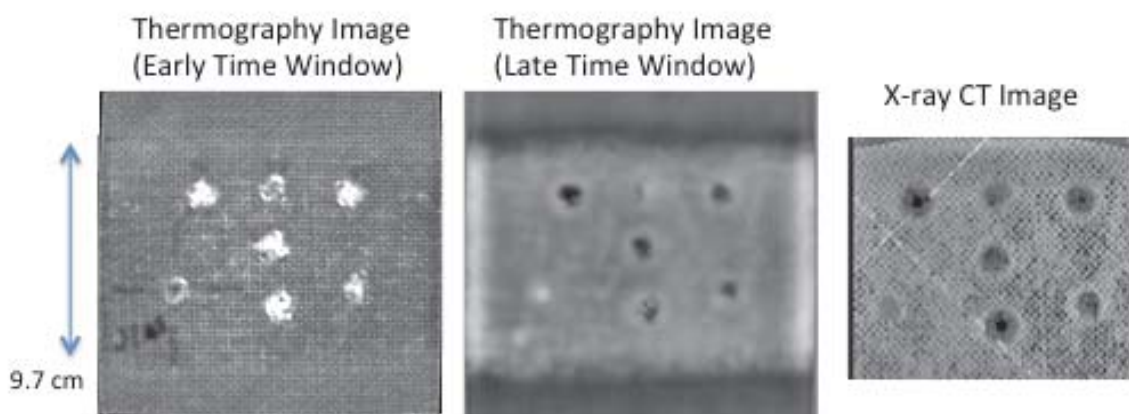


Figure 10. Thermography inspection results of early time (left image) and late time (middle image) of an impacted sandwich structure along with X-ray CT (right image).

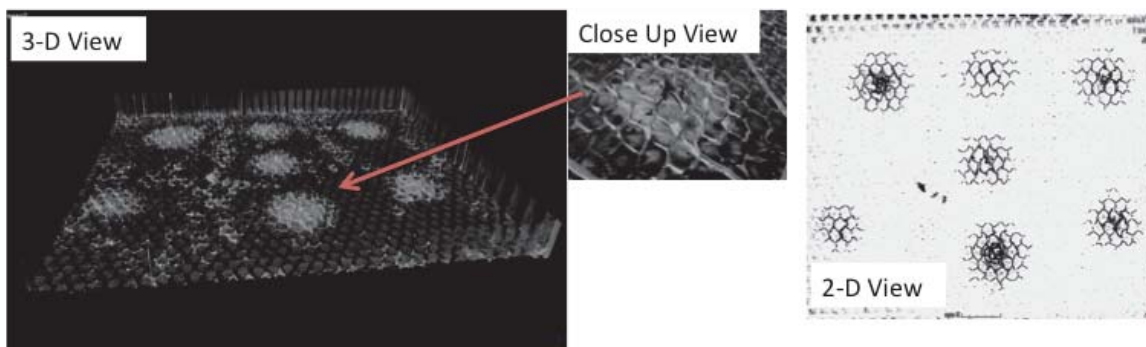


Figure 11. Images of the core crushed areas using X-ray CT.

Another sample, containing a face sheet crack, impact damage and core damage (cut core) was inspected. Shown in Figure 12 is an early time (0.33 – 1.5 seconds) PCA image of the honeycomb sample with a face sheet crack and impact damage defects. The bottom left image of Figure 12 is the late time (5.0 – 8.3 seconds) PCA image of the honeycomb sample showing the face sheet to core disbands along the edge. A later

start time (5.0 seconds) was used in the PCA processing to image the cut core areas and this was found to provide optimal results. The later time requirement is most likely due to some portion of the aluminum core still attached to the face sheet. This can be clearly seen in the left X-ray CT images of Figure 13 where some of the cut core is still attached to the face sheet and therefore later times were required to produce the surface temperature contrast. The attached core along with the resin fillet bonding changes the thermal response of the face sheet (more thickness) thus requiring a later start time to reveal contrast. Shown in Figure 13 is a close up area of the boxed region of Figure 12 where the impact damage is over an area of cut core. The early time image and late time image (shown in Figure 13) clearly reveals the face sheet impact damage and the face sheet to core disbond respectively. The face sheet to core disbond region is larger than the impact damage. The cut core cannot be detected under the impact damage area, as expected due to the delamination blocking the heat flow.

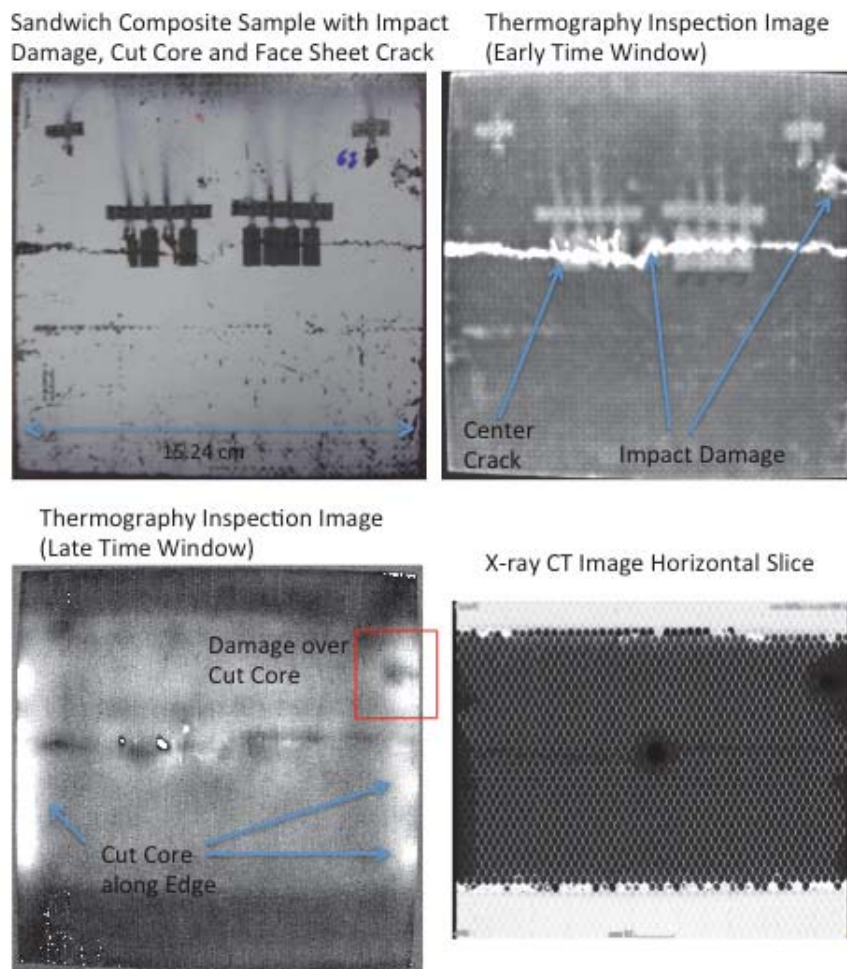


Figure 12. Thermography inspection results (early and late time) of the damaged sandwich panel with X-ray CT showing skin to core disbond.

Summary

Flash thermography and X-ray CT was used to detect defects in composite sandwich structures with an aluminum core. A thermal method was presented to detect damage in

aluminum core composite face sheet sandwich structures using PCA and time window analysis. The early time window PCA image using the first eigenvector was applied to detect face sheet impact damage. The late time window PCA image using the second eigenvector was applied to detect the face sheet to core disbond areas. The FEM analysis was helpful in selecting the eigenvector number and determining the optimal time windows. The flash thermography technique was not able to detect the core crushed areas. The X-ray CT inspection was able to detect impact damage, core crushed areas, and skin to core disbonds. The flash thermography results compared well with X-ray CT for impact damage detection and skin to core disbonds.

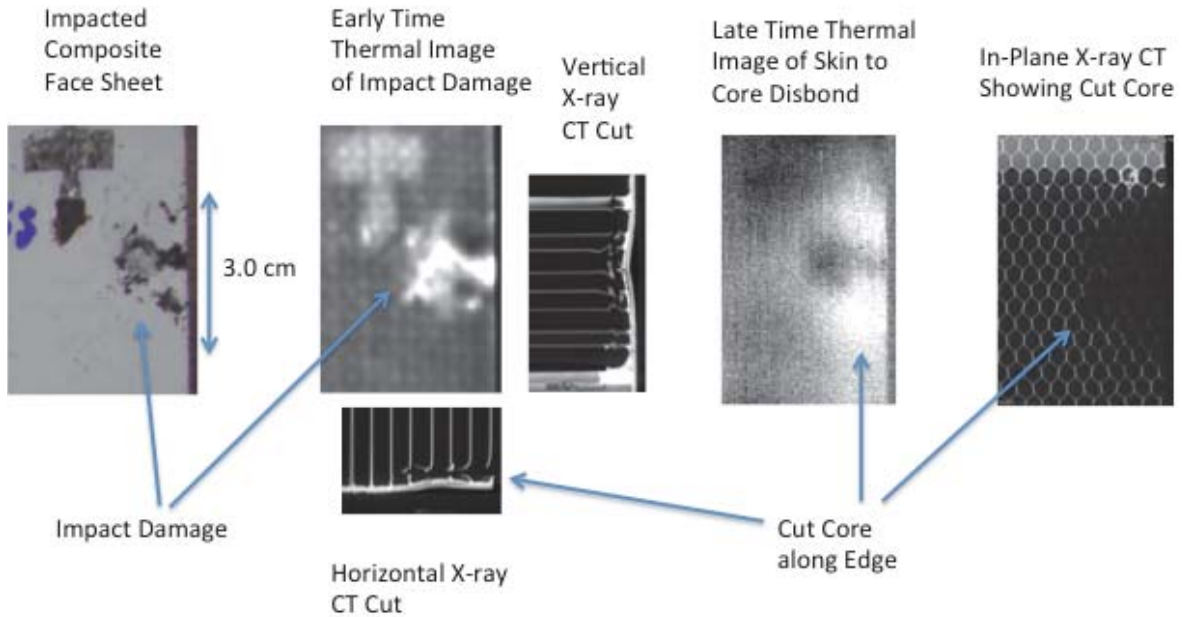


Figure 13. Thermography inspection close up of impact damage over cut core with X-ray CT.

References

1. Sfarra, S. *et al*, "[A comparative investigation for the nondestructive testing of honeycomb structures by holographic interferometry and infrared thermography](#)", *J. Phys.: Conf. Ser.* **214** 012071, (2010).
2. Clemente Ibarra-Castrando, et al, "Comparative Study of Active Thermography Techniques for the Nondestructive Evaluation of Honeycomb Structures", *Research in Nondestructive Evaluation* [Volume 20, Issue 1](#), (2009).
3. Genest, M., Brothers, M., Beltempo, C. A., Rutledge, R. S., "Nondestructive Evaluation of Aluminum Honeycomb Sandwich Structures", NATO Unclassified, STO-MP-AVT-224, (2013).
4. Liu, Tong, Malcolm, Andrew A., and Xu, Jian, "High Resolution X-ray CT Inspection of Honeycomb Composites Using Planar Computed Tomography Technology", 2nd International Symposium on NDT in Aerospace (2010).

5. Southward, T., Horrigan, D.P. W., Mallinson, G. D., and Jayaraman, K., "Failure of Sandwich Composite Structure Containing Face-sheet/Core Disbonds – An Experimental Study", 5th Australasian Congress on Applied Mechanics, ACAM 2007 10-12, Brisbane, Australia December (2007).
6. Zalameda, J. N., "Heat Source Finite Pulse Time Effects in Thermal Nondestructive Evaluation," *Materials Evaluation Journal*, American Society for Nondestructive Testing, Vol. 60, Nos.3, pp.425-429 March (2002).
7. Carslaw H. S. and Yeager J. C., [Conduction of Heat in Solids], 2nd. Ed. Oxford Univ. Press, (1959).
8. Talbot, A., *IMA J Appl Math* **23 (1)**: 97-120, (1979).
9. Shepherd, S. M., Lhota, J. M., and Ahmed, T., "Measurement Limits of Flash Thermography", *Proceedings of SPIE, Thermosense XXXI*, edited by Douglas D. Burleigh and Ralph B. Dinwiddie, Vol. 7299, (2009).
10. Devadas, N. P., Sunilkumar, G., and Sajeeb, R., "Finite Element Analysis of Flat Joints in Metallic Honeycomb Sandwich Beams", *Journal of Mechanical and Civil Engineering*, ISSN: 2278-1684, Vol. 3, Issue 2, Sept-Oct. (2011).
11. LISA Finite Element Analysis, software version 8.0.0, (2013).
12. Rajic, N., "Principal Component Thermography for Flaw Contrast Enhancement and Flaw Depth Characterisation in Composite Structures", *Composite Structures*, Vol. 58, pp. 521--528, (2002).
13. Cramer, K. E. and Winfree, W. P., "Fixed Eigenvector Analysis of Thermographic NDE Data", *Proceedings of SPIE, Thermosense XXXIII*, edited by Morteza Safai and Jeff Brown, Vol. 8013, (2011).

REPORT DOCUMENTATION PAGE

*Form Approved
OMB No. 0704-0188*

The public reporting burden for this collection of information is estimated to average 1 hour per response, including the time for reviewing instructions, searching existing data sources, gathering and maintaining the data needed, and completing and reviewing the collection of information. Send comments regarding this burden estimate or any other aspect of this collection of information, including suggestions for reducing this burden, to Department of Defense, Washington Headquarters Services, Directorate for Information Operations and Reports (0704-0188), 1215 Jefferson Davis Highway, Suite 1204, Arlington, VA 22202-4302. Respondents should be aware that notwithstanding any other provision of law, no person shall be subject to any penalty for failing to comply with a collection of information if it does not display a currently valid OMB control number.
PLEASE DO NOT RETURN YOUR FORM TO THE ABOVE ADDRESS.

1. REPORT DATE (DD-MM-YYYY) 01-11-2014		2. REPORT TYPE Technical Memorandum		3. DATES COVERED (From - To)	
4. TITLE AND SUBTITLE Nondestructive Evaluation (NDE) for Inspection of Composite Sandwich Structures				5a. CONTRACT NUMBER	
				5b. GRANT NUMBER	
				5c. PROGRAM ELEMENT NUMBER	
6. AUTHOR(S) Zalameda, Joseph N.; Parker, F. Raymond				5d. PROJECT NUMBER	
				5e. TASK NUMBER	
				5f. WORK UNIT NUMBER 724297.40.44.07	
7. PERFORMING ORGANIZATION NAME(S) AND ADDRESS(ES) NASA Langley Research Center Hampton, VA 23681-2199				8. PERFORMING ORGANIZATION REPORT NUMBER L-20480	
9. SPONSORING/MONITORING AGENCY NAME(S) AND ADDRESS(ES) National Aeronautics and Space Administration Washington, DC 20546-0001				10. SPONSOR/MONITOR'S ACRONYM(S) NASA	
				11. SPONSOR/MONITOR'S REPORT NUMBER(S) NASA/TM-2014-218545	
12. DISTRIBUTION/AVAILABILITY STATEMENT Unclassified - Unlimited Subject Category 39 Availability: NASA CASI (443) 757-5802					
13. SUPPLEMENTARY NOTES					
14. ABSTRACT Composite honeycomb structures are widely used in aerospace applications due to their low weight and high strength advantages. Developing nondestructive evaluation (NDE) inspection methods are essential for their safe performance. Flash thermography is a commonly used technique for composite honeycomb structure inspections due to its large area and rapid inspection capability. Flash thermography is shown to be sensitive for detection of face sheet impact damage and face sheet to core disbond. Data processing techniques, using principal component analysis to improve the defect contrast, are discussed. Limitations to the thermal detection of the core are investigated. In addition to flash thermography, X-ray computed tomography is used. The aluminum honeycomb core provides excellent X-ray contrast compared to the composite face sheet. The X-ray CT technique was used to detect impact damage, core crushing, and skin to core disbonds. Additionally, the X-ray CT technique is used to validate the thermography results.					
15. SUBJECT TERMS Aluminum; Composite; Inspection; Nondestructive test; Structures					
16. SECURITY CLASSIFICATION OF:			17. LIMITATION OF ABSTRACT	18. NUMBER OF PAGES	19a. NAME OF RESPONSIBLE PERSON
a. REPORT	b. ABSTRACT	c. THIS PAGE			STI Help Desk (email: help@sti.nasa.gov)
U	U	U	UU	17	19b. TELEPHONE NUMBER (Include area code) (443) 757-5802